Proceedings of the 7th Mediterranean Conference on Control and Automation (MED99) Haifa, Israel - June 28-30, 1999

On the Inclusion of Robot Dynamics in Visual Servoing Systems

Fabio Conticelli* Benedetto Allotta†
PERCRO Lab
Scuola Superiore Sant'Anna
Via Carducci 40, I-56127 Pisa, ITALY
tel +39-50-883445
fax +39-50-883210

Abstract

In this paper the problem of including the robot dynamics in the control loop of visual servoing systems is considered. After introducing the image-based visual interaction model between a robot camera and a rigid object parametrized by a finite number of image features, the problem of local feedback stabilization is considered, in both the cases of interconnection to a linear subsystem and to a nonlinear open-chain manipulator. The proposed control system design uses backstepping approach to ensure local stablity of the equilibrium of the whole system, assuming that the linear subsystem is minimum phase of relative degree one. In the case of inclusion of the nonlinear lagrangian dynamics of the robot, the obtained control law is similar to the well-known computed torque law. A case study is also reported to validate the developed control design, approximating the robot and its local controller by a diagonal linear subsystem.

1 Introduction

Image-based visual servo systems (Hill and Park, 1979) permit to control the relative pose between a robot camera and a finite number of image features which parametrize a visual target. In image-based servoing (Weiss *et al.*, 1987), any visual task is described in the image plane as a desired evolution of image features towards a goal one. Even if image-based systems have been largely investigated (Feddema and Mitchell, 1989; Espiau *et al.*, 1992; Grosso *et al.*, 1996; Hashimoto *et al.*, 1996; Colombo and Allotta, 1999) and they are now well established, few approaches have been proposed to include explicitely the robot dynamics in the visual servo loop. In (Papanikolopoulos and Khosla, 1993), the visual servo system consists in a camera mounted on the wrist of a PUMA robot, and a PD scheme with gravity compensation is used to compute the actuated joints torques of the manipulator. In (Corke and Good, 1996), a PUMA robot is used as a pan/tilt head to realize high-performance visual feedback, dynamic effects are taken into account by modeling the inner position/velocity loop of the robot. In (Kelly *et al.*, 1997), the lagrangian dynamics of the manipulator are included in the visual servo design, the authors consider the case of a planar robot with a fixed camera viewing the robot workspace.

In this paper, the problem of the inclusion of robot dynamics in the control loop of the visual system is solved by applying backstepping approach. The dynamic visual model of interaction

*Email: *contice@sssup.it*
†Email: *ben@sssup.it*

between the robot camera and the image features parameters is viewed as a smooth input-affine nonlinear system. Assuming the existence of a local smooth stabilizing control law for the visual system, the stabilization of the interconnected system including the robot dynamics is addressed. Two architectures are considered: dynamic look-and-move systems and direct visual servos. In the first case, the controller realizes an outer loop, it generates a twist screw fed to an inner position/velocity controller, the robot dynamics compensated with the local controller is modeled as a linear subsystem, whose effects are included in the visual loop. In the case of direct visual servos, the image-based controller provides directly the robot joint torques, and the full lagrangian dynamics of the open-chain manipulator is included explicitly in the control system design. The designed control system ensures Lyapunov stability and convergence to a local invariant set in the state space. Sufficient conditions which guarantee local and global asymptotic stability around the set of desired image features are also discussed. A case study is reported to validate the developed approach. The problem of controlling the pose of the robot camera mounted on a 6-DOF manipulator with respect to a rigid object is addressed, by using the proposed control system design. The robot and its local controller are modeled as a diagonal linear subsystem.

The paper is organized as follows. In Sect. 2, visual modeling issues are considered, by introducing the dynamic interaction model. In Sect. 3, the control system is designed and stability analysis is carried out. Sect. 4 reports an application of the proposed approach, simulation results are carried out to validate the framework. Finally, in Sect. 5 the major contribution of the paper is summarized.

2 Image-Based Visual Modeling

Consider a rigid object of interest, which is in the visual field of the camera, denote with γ the projection in the image plane of the object's visible surface Γ, i.e $\gamma = \pi(\Gamma)$, where π denotes a camera projection model (e.g. full perspective, para-pespective, orthographic (Mundy and Zisserman, 1992)). Assume that the image patch γ can be parametrized by a finite number of geometrical features $\boldsymbol{p} = [p_1, \ldots, p_{n_p}]^{\mathrm{T}}$, $\boldsymbol{p} \in \mathcal{P}$, which are, in general, image points. Let us associate to γ a finite number of image features, they are real-valued quantities algebrically computed from one or more geometrical features, i.e $\boldsymbol{w} = \boldsymbol{s}_p(\boldsymbol{p})$, being $\boldsymbol{s}_p$ a smooth map. Examples of image features used in the letterature are image points (Papanikolopoulos and Khosla, 1993; Castano and Hutchinson, 1994; Hashimoto *et al.*, 1996), parameters of geometrical primitives (line, plane, circle, ellipse) in the image plane (Espiau *et al.*, 1992), and area of the projected surface (Weiss *et al.*, 1987). Assume that the set of image features is a smooth manifold $\mathcal{W}$ of dimension $n_w \leq 6$, let us indicate with $\boldsymbol{w} = [w_1, \ldots, w_{n_w}]^{\mathrm{T}}$ the local coordinates of an element w of $\mathcal{W}$. Let $\mathcal{D}$ be an open subset of $SE(3)$, the Special Euclidean group, and assume that the two set $\mathcal{W}$ and $\mathcal{D}$ are smooth diffeomophic manifolds. Hence, there exists a smooth map $F : \mathcal{D} \to \mathcal{W}$, such that $\forall d \in \mathcal{D}$, there exists coordinate chart (D, ϕ) of $\mathcal{D}$ and (W, ψ) of $\mathcal{W}$, with $d \in D$, and $F(d) \in \mathcal{W}$. The dynamic visual model of interaction can be, in principle, computed considering the tangent map F_{*d} of F at d, in local coordinates results:

$$\dot{\boldsymbol{w}} = \frac{\partial(\psi \circ F \circ \phi^{-1})}{\partial \boldsymbol{d}} \dot{\boldsymbol{d}} \quad , \tag{1}$$

where $\frac{\partial(\psi \circ F \circ \phi^{-1})}{\partial \boldsymbol{d}}$ is the analytic image jacobian of the system, and $\boldsymbol{d} \in \Re^{n_d}$ are local coordinated of an element of $\mathcal{D}$. Since the expression of the map F is usually unknown or too complicated to be used (it is related to the problem of calibration of the visual system), the dynamic visual

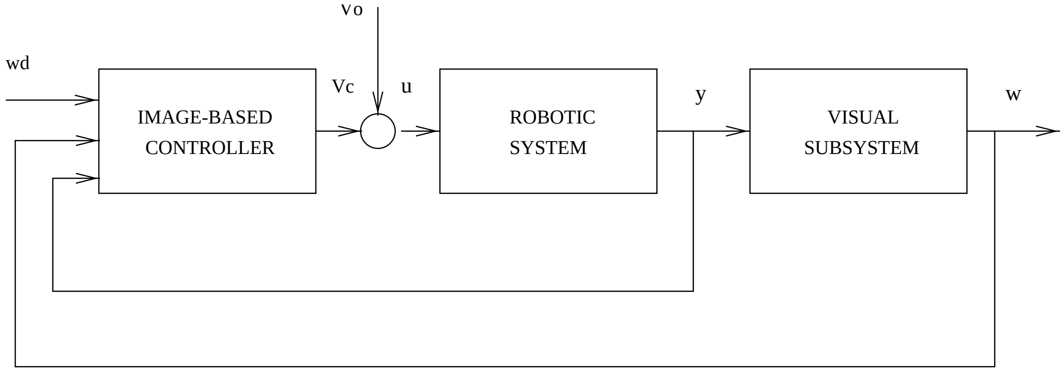

Figure 1: Block diagramm of the image-based servoing system.

model is usually derived geometrically, by using the optical flow equations (Koenderink, 1986): $\dot{\boldsymbol{p}}_i = U(\boldsymbol{p}_i, z_i)\,\boldsymbol{u}$, where $\boldsymbol{p}_i = \pi(\boldsymbol{P}_i)$ is the projection of the cartesian point $\boldsymbol{P}_i$ according π. z_i is the depth of the point $\boldsymbol{P}_i$, and $\boldsymbol{u}$ is the vector of relative twist coordinates between camera and object. Then, by using the algebric relation between the image features and geometrical features, the dynamic visual model can be expressed in the form:

$$\dot{\boldsymbol{w}} = \sum_{i=1}^{n_p} \frac{\partial \boldsymbol{s_p}}{\partial \boldsymbol{p}_i} U(\boldsymbol{p}_i, z_i)\,\boldsymbol{u} \quad . \tag{2}$$

Even if in some cases the relation between the image and geometrical features is expressed in the implicit form $\boldsymbol{s_p}(\boldsymbol{w}, \boldsymbol{p}) = 0$, the dynamic model of interaction can be still derived (see (Espiau *et al.*, 1992)). The image-based visual model is a smooth input-affine nonlinear system $\dot{\boldsymbol{w}} = G(\boldsymbol{w}, \boldsymbol{z})\,\boldsymbol{u}$, defined on the smooth manifold $\mathcal{W}$, with time-varying parameters $\boldsymbol{z} = [z_1, \ldots, z_{n_p}]^{\mathrm{T}}$, and which is without the drift term. Visual interaction model with drift can be also considered by extending the dynamics (2), in order to derive a model which include also the velocity of image features as state variables, i.e. defined in the tangent bundle $\mathcal{W} \times T_{\boldsymbol{w}}\mathcal{W}$ (see (Conticelli and Allotta, 1998) for an example). The visual model is, in general, of the form $\dot{\boldsymbol{w}} = \boldsymbol{f}(\boldsymbol{w}) + G(\boldsymbol{w})\,\boldsymbol{u}$, denote with $\boldsymbol{w}^{(\mathrm{d})}$ the desired constant state, in the error coordinate $\boldsymbol{x} = \boldsymbol{w} - \boldsymbol{w}^{(\mathrm{d})}$ the visual subsystem has equation: $\dot{\boldsymbol{x}} = \boldsymbol{f}(\boldsymbol{x}) + G(\boldsymbol{x})\,\boldsymbol{u}$. In the next section, we use the following assumption.

Assumption 1 *There exists a local smooth stabilizing feedback:* $\boldsymbol{y} = \boldsymbol{\alpha}(\boldsymbol{x})$, $\boldsymbol{\alpha}(\boldsymbol{0}) = \boldsymbol{0}$, *and a function* $V(\boldsymbol{x}) : \Re^m \to \Re$ *such that the region* $\Omega_l(\boldsymbol{x}) = \{\boldsymbol{x} \in \Re^m : V(\boldsymbol{x}) < l\}$, $l > 0$, *is bounded, and* $\frac{\partial V(\boldsymbol{x})}{\partial \boldsymbol{x}}(\boldsymbol{f}(\boldsymbol{x}) + G(\boldsymbol{x})\boldsymbol{\alpha}(\boldsymbol{x})) \leq 0$, $\forall \boldsymbol{x} \in \Omega_l$.

The feedback law $\boldsymbol{\alpha}(\boldsymbol{x})$ locally stabilizes the equilibrium $\boldsymbol{x} = \boldsymbol{0}$ in the sense of Lyapunov, by applying La Salle theorem.

3 Backstepped Visual Servoing

In this section, we consider both the cases of dynamic look-and-move and direct visual servo systems. The backstepping approach is used to construct control laws which include the robot dynamics in the visual servo loop.

3.1 Dynamic Look-and-Move Systems

In the case of dynamic look-and-move systems, the robotic system (see Fig. (1)) consists in the dynamics of the manipulator and a local position/velocity controller. It is assumed that the latter permits to compensate the nonlinear dynamics of the manipulator, such that the composition of the two systems can be described by a linear subsystem. The following proposition provides a control system design taking into account both the linear subsystem and the dynamic visual model of interaction (visual subsystem). The control system generates the velocity twist of the camera fed to the position/velocity inner loop of the robot.

Proposition 1 *Consider the interconnected system:*

$$\begin{aligned} \dot{\boldsymbol{x}} &= \boldsymbol{f}(\boldsymbol{x}) + G(\boldsymbol{x})\boldsymbol{y} \\ \dot{\boldsymbol{\xi}} &= A\boldsymbol{\xi} + B\boldsymbol{u} \\ \boldsymbol{y} &= H\boldsymbol{\xi} \quad , \end{aligned} \tag{3}$$

where $\boldsymbol{x} \in \Re^m$ is the state of the visual subsystem, $\boldsymbol{y} \in \Re^p$ is the velocity screw of the camera, $\boldsymbol{\xi} \in \Re^n$ is the state of the linear subsystem, and $\boldsymbol{u} \in \Re^p$ is the robot command. Assume that:

- *(1) holds;*
- *the linear subsystem is minimum phase of vector relative degree $\{1, \ldots, 1\}$;*

by using the control law:

$$\boldsymbol{u} = (HB)^{-1}[-K(\boldsymbol{y} - \boldsymbol{\alpha}(\boldsymbol{x})) - G(\boldsymbol{x})^T(\frac{\partial V(\boldsymbol{x})}{\partial \boldsymbol{x}})^T - HA\boldsymbol{\xi} + \dot{\boldsymbol{\alpha}}(\boldsymbol{x})] \quad , \tag{4}$$

where the matrix K is positive definite, then the state of the whole system $[\boldsymbol{x}^T,\ \boldsymbol{\xi}^T]^T$ is locally bounded and converges to the largest invariant set contained in $M(\boldsymbol{x}, \boldsymbol{\xi}) = \{[\boldsymbol{x}^T,\ \boldsymbol{\xi}^T]^T : \dot{V}(\boldsymbol{x}) = 0,\ \boldsymbol{y} = \boldsymbol{\alpha}(\boldsymbol{x})\}$. Moreover, if $\frac{\partial V(\boldsymbol{x})}{\partial \boldsymbol{x}}(\boldsymbol{f}(\boldsymbol{x}) + G(\boldsymbol{x})\boldsymbol{\alpha}(\boldsymbol{x})) < 0$, then the equilibrium $[\boldsymbol{x}^T,\ \boldsymbol{\xi}^T]^T = \boldsymbol{0}$ is locally asymptotically stable.

Proof:
By using system theory (Isidori, 1989), there exists a linear change of coordinates which put the linear subsystem in the normal form:

$$\begin{aligned} \dot{\boldsymbol{y}} &= HA\,\boldsymbol{\xi} + HB\,\boldsymbol{u} \\ \dot{\boldsymbol{\mu}} &= A_0\,\boldsymbol{\mu} + B_0\,\boldsymbol{y} \quad , \end{aligned} \tag{5}$$

where $\boldsymbol{\mu} \in \Re^{n-p}$, and the matrix A_0, which defines the zero dynamics, is Hurwitz by assumption. It is easy to prove that the required diffeomorphism is $\boldsymbol{\phi}(\boldsymbol{\xi}) = [y_1, \ldots, y_p, \sigma_1\boldsymbol{\xi}, \ldots, \sigma_{n-p}\boldsymbol{\xi}]$, where $\sigma_i^{\mathrm{T}} \in \Re^n,\ i = 1, \ldots, n-p$ is a basis of $\mathrm{Ker\,B^T}$. Consider the semi-positive definite function:

$$V_a(\boldsymbol{x}, \boldsymbol{\xi}) = V(\boldsymbol{x}) + (\boldsymbol{y} - \boldsymbol{\alpha}(\boldsymbol{x}))^{\mathrm{T}}(\boldsymbol{y} - \boldsymbol{\alpha}(\boldsymbol{x})) \quad , \tag{6}$$

The first derivative of $V_a(\boldsymbol{x}, \boldsymbol{\xi})$, by using (4), results:

$$\begin{aligned} \dot{V}_a(\boldsymbol{x}, \boldsymbol{\xi}) &= \frac{\partial V(\boldsymbol{x})}{\partial \boldsymbol{x}}(\boldsymbol{f}(\boldsymbol{x}) + G(\boldsymbol{x})\boldsymbol{y}) + (\boldsymbol{y} - \boldsymbol{\alpha}(\boldsymbol{x}))^{\mathrm{T}}(H\,A\boldsymbol{\xi} + H\,B\boldsymbol{u} - \dot{\boldsymbol{\alpha}}(\boldsymbol{x})) \\ &= \frac{\partial V(\boldsymbol{x})}{\partial \boldsymbol{x}}(\boldsymbol{f}(\boldsymbol{x}) + G(\boldsymbol{x})\boldsymbol{\alpha}(\boldsymbol{x})) + (\boldsymbol{y} - \boldsymbol{\alpha}(\boldsymbol{x}))^{\mathrm{T}}(G(\boldsymbol{x})^{\mathrm{T}}(\frac{\partial V(\boldsymbol{x})}{\partial \boldsymbol{x}})^{\mathrm{T}} + HA\boldsymbol{\xi} + HB\boldsymbol{u} - \dot{\boldsymbol{\alpha}}(\boldsymbol{x})) \\ &\leq -(\boldsymbol{y} - \boldsymbol{\alpha}(\boldsymbol{x}))^{\mathrm{T}}\,K(\boldsymbol{y} - \boldsymbol{\alpha}(\boldsymbol{x})) \quad , \end{aligned} \tag{7}$$

which is semi-negative definite. Notice that, since the linear subsystem has vector relative degree $\{1,\ldots,1\}$ the matrix $(H\,B)$ is nonsingular. It follows that the variables $\boldsymbol{x}$, and $\boldsymbol{y}$ are locally bounded. Moreover, since A_0 is Hurwitz, then $\boldsymbol{\mu}$ is also bounded. By applying La Salle theorem, the whole state $[\boldsymbol{x}^{\mathrm{T}},\ \boldsymbol{\xi}^{\mathrm{T}}]^{\mathrm{T}}$ converges to the largest invariant set contained in $M(\boldsymbol{x},\boldsymbol{\xi})$. Notice that the control law (4) can be written in the form $\boldsymbol{u} = (HB)^{-1}(\nu - HA\boldsymbol{\xi})$, where the vector ν is obviously defined. Hence, the subsystem:

$$\begin{aligned} \dot{\boldsymbol{x}} &= \boldsymbol{f}(\boldsymbol{x}) + G(\boldsymbol{x})\boldsymbol{y} \\ \dot{\boldsymbol{y}} &= \nu \quad , \end{aligned} \tag{8}$$

can be decoupled from the internal dynamics $\dot{\boldsymbol{\mu}} = A_0\boldsymbol{\mu} + B_0\boldsymbol{y}$. Consider the definite positive function (6), defined in the state $[\boldsymbol{x}^{\mathrm{T}},\boldsymbol{y}^{\mathrm{T}}]^{\mathrm{T}}$, and by using the fact that $\frac{\partial V(\boldsymbol{x})}{\partial \boldsymbol{x}}(\boldsymbol{f}(\boldsymbol{x})+G(\boldsymbol{x})\boldsymbol{\alpha}(\boldsymbol{x})) < 0$, the first derivative of $V_a(\boldsymbol{x},\boldsymbol{y})$ results negative definite, infact $\dot{V}_a(\boldsymbol{x},\boldsymbol{y}) < -(\boldsymbol{y}-\boldsymbol{\alpha}(\boldsymbol{x}))^{\mathrm{T}}\,K(\boldsymbol{y}-\boldsymbol{\alpha}(\boldsymbol{x})) \leq 0$. It follows that the equilibrium $[\boldsymbol{x}^{\mathrm{T}},\ \boldsymbol{y}^{\mathrm{T}}]^{\mathrm{T}} = \boldsymbol{0}$ is locally asymptotically stable. Finally, since A_0 is Hurwitz, it is simple to show (see (Krstić *et al.*, 1995)) that the internal dynamics is also asymptotically stable, which concludes the proof.

Remark 1 *Assume also that* $V(\boldsymbol{x})$ *is radially unbounded and* $\frac{\partial V(\boldsymbol{x})}{\partial \boldsymbol{x}}(\boldsymbol{f}(\boldsymbol{x}) + G(\boldsymbol{x})\boldsymbol{\alpha}(\boldsymbol{x})) \leq 0$, $\forall \boldsymbol{x} \in \Re^m$, *by applying the Global Invariant Set Theorem (Slotine and Li, 1993), the state of the whole system* $[\boldsymbol{x}^T,\ \boldsymbol{\xi}^T]^T$ *is globally bounded and converges to the largest invariant set contained in* $M(\boldsymbol{x},\boldsymbol{\xi})$. *Moreover, if* $\frac{\partial V(\boldsymbol{x})}{\partial \boldsymbol{x}}(\boldsymbol{f}(\boldsymbol{x})+G(\boldsymbol{x})\boldsymbol{\alpha}(\boldsymbol{x})) < 0$, *then the equilibrium* $[\boldsymbol{x}^T,\ \boldsymbol{\xi}^T]^T = \boldsymbol{0}$ *is globally asymptotically stable.*

Remark 2 *Assume that the inner loop decouples the robot dynamics such that each degree of freedom of the robot can be modeled by a SISO (single input - single output) linear subsystem of the form:*

$$\begin{aligned} \dot{y}_i &= h_i A_i\,\boldsymbol{\xi}_i + h_i b_i\,u_i \\ \dot{\boldsymbol{\mu}}_i &= A_{0_i}\,\boldsymbol{\mu}_i + b_{0_i}\,y_i,\ \ i = 1,\ldots,N \quad , \end{aligned} \tag{9}$$

where N *is the number of degrees of freedom. If each linear subsystem is minimum phase and has relative degree 1, then the diagonal linear subsystem obtained by stacking the Eqs. (9) is also minimum phase and has vector relative degree* $\{1,\ldots,1\}$ *by construction, hence it satisfies the assumption of Prop. 1.*

3.2 Direct Visual Servo Systems

In the case of direct visual servo systems, the robotic system (see Fig. (1)) consists in the dynamics of the manipulator, without any local position controller. The following proposition provides a control system design taking into account both the nonlinear dynamics of the manipulator and the dynamic visual model of interaction (visual subsystem). The control system generates directly the joints actuator torques.

Proposition 2 *Consider the interconnected system:*

$$\begin{aligned} \dot{\boldsymbol{x}} &= \boldsymbol{f}(\boldsymbol{x}) + G(\boldsymbol{x})\boldsymbol{y} \\ A(\boldsymbol{q})\ddot{\boldsymbol{q}} &+ B(\boldsymbol{q},\dot{\boldsymbol{q}})\dot{\boldsymbol{q}} + C(\boldsymbol{q}) = \boldsymbol{\tau} \\ \boldsymbol{y} &= J(\boldsymbol{q})\dot{\boldsymbol{q}} \quad , \end{aligned} \tag{10}$$

where $\boldsymbol{x} \in \Re^m$ *is the state of the visual subsystem,* $\boldsymbol{y} \in \Re^p$ *is the velocity screw of the camera,* $\boldsymbol{q}$, $\dot{\boldsymbol{q}} \in \Re^n$ *are respectively the robot joints angles and their velocities,* $\boldsymbol{\tau} \in \Re^p$ *is the vector of actuator torques,* $A(\boldsymbol{q})$ *is the inertial matrix of the robot,* $B(\boldsymbol{q}, \dot{\boldsymbol{q}})$ *is the Coriolis matrix, and* $C(\boldsymbol{q})$ *is the gravity term. Assume that:*

- *(1) holds;*
- *each joint of the robot is actuated, and the robot system is square i.e.* $n = s = p$*;*

by using the control law:

$$\boldsymbol{\tau} = A(\boldsymbol{q})[-K(\dot{\boldsymbol{q}} - \overline{\boldsymbol{\alpha}}(\boldsymbol{x}, \boldsymbol{q})) - J(\boldsymbol{q})^T G(\boldsymbol{x})^T (\frac{\partial V(\boldsymbol{x})}{\partial \boldsymbol{x}})^T + \dot{\overline{\boldsymbol{\alpha}}}(\boldsymbol{x}, \boldsymbol{q}))] + B(\boldsymbol{q}, \dot{\boldsymbol{q}})\dot{\boldsymbol{q}} + C(\boldsymbol{q}) \quad , \qquad (11)$$

where the matrix K *is positive definite, and* $\overline{\boldsymbol{\alpha}}(\boldsymbol{x}, \boldsymbol{q}) = J(\boldsymbol{q})^{-1}\boldsymbol{\alpha}(\boldsymbol{x})$*, then the state of the whole system* $[\boldsymbol{x}^T,\ \boldsymbol{q}^T,\ \dot{\boldsymbol{q}}^T]^T$ *is locally bounded and converges to the largest invariant set contained in* $M(\boldsymbol{x}, \boldsymbol{q}, \dot{\boldsymbol{q}}) = \{[\boldsymbol{x}^T,\ \boldsymbol{q}^T,\ \dot{\boldsymbol{q}}^T]^T : \dot{V}(\boldsymbol{x}) = 0,\ \dot{\boldsymbol{q}} = \overline{\boldsymbol{\alpha}}(\boldsymbol{x}, \boldsymbol{q})\}$*. Moreover, if* $\frac{\partial V(\boldsymbol{x})}{\partial \boldsymbol{x}}(\boldsymbol{f}(\boldsymbol{x}) + G(\boldsymbol{x})\boldsymbol{\alpha}(\boldsymbol{x})) < 0$*, then the equilibrium* $[\boldsymbol{x}^T,\ \boldsymbol{q}^T,\ \dot{\boldsymbol{q}}^T]^T = [\boldsymbol{0},\ \boldsymbol{q}^{T\,*},\ \boldsymbol{0}]^T$ *is locally asymptotically stable, where* $\boldsymbol{q}^*$ *is the robot configuration corresponding to* $\boldsymbol{x} = \boldsymbol{0}$*.*

Proof:
Consider as output of the robot system the joints angles, from Eq. (10), it follows that $\ddot{\boldsymbol{q}} = A(\boldsymbol{q})^{-1}(\boldsymbol{\tau} - B(\boldsymbol{q}, \dot{\boldsymbol{q}})\dot{\boldsymbol{q}} - C(\boldsymbol{q}))$, and, since $\det A(\boldsymbol{q}) \neq 0,\ \forall \boldsymbol{q} \in \Re^n$, the robot has vector relative degree $\{2,\ldots,2\}$, which implies that the total relative degree is equal to the dimension of the robot state space, hence there is no internal dynamics. Consider the semi-positive definite function:

$$V_a(\boldsymbol{x}, \boldsymbol{q}, \dot{\boldsymbol{q}}) = V(\boldsymbol{x}) + (\dot{\boldsymbol{q}} - \overline{\boldsymbol{\alpha}}(\boldsymbol{x}, \boldsymbol{q}))^{\mathrm{T}}(\dot{\boldsymbol{q}} - \overline{\boldsymbol{\alpha}}(\boldsymbol{x}, \boldsymbol{q})) \quad , \qquad (12)$$

The first derivative of $V_a(\boldsymbol{x}, \boldsymbol{q}, \dot{\boldsymbol{q}})$, by using (11), results:

$$\begin{aligned}
\dot{V}_a(\boldsymbol{x}, \boldsymbol{q}, \dot{\boldsymbol{q}}) &= \frac{\partial V(\boldsymbol{x})}{\partial \boldsymbol{x}}(\boldsymbol{f}(\boldsymbol{x}) + G(\boldsymbol{x})\boldsymbol{y}) + (\dot{\boldsymbol{q}} - \overline{\boldsymbol{\alpha}}(\boldsymbol{x}, \boldsymbol{q}))^{\mathrm{T}}(\ddot{\boldsymbol{q}} - \dot{\overline{\boldsymbol{\alpha}}}(\boldsymbol{x}, \boldsymbol{q})) \\
&= \frac{\partial V(\boldsymbol{x})}{\partial \boldsymbol{x}}(\boldsymbol{f}(\boldsymbol{x}) + G(\boldsymbol{x})\boldsymbol{\alpha}(\boldsymbol{x})) + (\dot{\boldsymbol{q}} - \overline{\boldsymbol{\alpha}}(\boldsymbol{x}, \boldsymbol{q}))^{\mathrm{T}} \\
&\quad (\ddot{\boldsymbol{q}} - \dot{\overline{\boldsymbol{\alpha}}}(\boldsymbol{x}, \boldsymbol{q}) + J(\boldsymbol{q})^{\mathrm{T}} G(\boldsymbol{x})^{\mathrm{T}}(\frac{\partial V(\boldsymbol{x})}{\partial \boldsymbol{x}})^{\mathrm{T}})) \leq (\dot{\boldsymbol{q}} - \overline{\boldsymbol{\alpha}}(\boldsymbol{x}, \boldsymbol{q}))^{\mathrm{T}}(A(\boldsymbol{q})^{-1}(\boldsymbol{\tau} - B(\boldsymbol{q}, \dot{\boldsymbol{q}})\dot{\boldsymbol{q}} \\
&\quad -C(\boldsymbol{q})) - \dot{\overline{\boldsymbol{\alpha}}}(\boldsymbol{x}, \boldsymbol{q}) + J(\boldsymbol{q})^{\mathrm{T}} G(\boldsymbol{x})^{\mathrm{T}}(\frac{\partial V(\boldsymbol{x})}{\partial \boldsymbol{x}})^{\mathrm{T}}) \leq -(\dot{\boldsymbol{q}} - \overline{\boldsymbol{\alpha}}(\boldsymbol{x}, \boldsymbol{q}))^{\mathrm{T}} K(\dot{\boldsymbol{q}} - \overline{\boldsymbol{\alpha}}(\boldsymbol{x}, \boldsymbol{q})) \quad , (13)
\end{aligned}$$

which is semi-negative definite. It follow that the whole state of the interconnected system $[\boldsymbol{x}^{\mathrm{T}},\ \boldsymbol{q}^{\mathrm{T}},\ \dot{\boldsymbol{q}}]^{\mathrm{T}}$ is locally bounded. By applying La Salle theorem, the whole state converges to the largest invariant set contained in $M(\boldsymbol{x}, \boldsymbol{q}, \dot{\boldsymbol{q}})$. Assume that $\frac{\partial V(\boldsymbol{x})}{\partial \boldsymbol{x}}(\boldsymbol{f}(\boldsymbol{x}) + G(\boldsymbol{x})\boldsymbol{\alpha}(\boldsymbol{x})) < 0$, the first derivative of $V_a(\boldsymbol{x}, \boldsymbol{q}, \dot{\boldsymbol{q}})$ results: $\dot{V}_a(\boldsymbol{x}, \boldsymbol{q}, \dot{\boldsymbol{q}}) < -(\dot{\boldsymbol{q}} - \overline{\boldsymbol{\alpha}}(\boldsymbol{x}, \boldsymbol{q}))^{\mathrm{T}} K(\dot{\boldsymbol{q}} - \overline{\boldsymbol{\alpha}}(\boldsymbol{x}, \boldsymbol{q})) \leq 0$, then, by La Salle theorem, the whole state converges to the largest invariant set contained in $\{[\boldsymbol{x}^{\mathrm{T}},\ \boldsymbol{q}^{\mathrm{T}},\ \dot{\boldsymbol{q}}]^{\mathrm{T}} :\ \dot{\boldsymbol{q}} = \overline{\boldsymbol{\alpha}}(\boldsymbol{x}, \boldsymbol{q})\}$. The following argumentation proves that this invariant set is simply the point $[\boldsymbol{x}^{\mathrm{T}},\ \boldsymbol{q}^{\mathrm{T}},\ \dot{\boldsymbol{q}}^{\mathrm{T}}]^{\mathrm{T}} = [\boldsymbol{0},\ \boldsymbol{q}^{\mathrm{T}\,*},\ \boldsymbol{0}]^{\mathrm{T}}$, where $\boldsymbol{q}^*$ is the robot configuration corresponding to $\boldsymbol{x} = \boldsymbol{0}$. Since $\frac{\partial V(\boldsymbol{x})}{\partial \boldsymbol{x}}(\boldsymbol{f}(\boldsymbol{x}) + G(\boldsymbol{x})\boldsymbol{\alpha}(\boldsymbol{x})) < 0$, it follows that $\boldsymbol{x} \to 0$, which implies that $\boldsymbol{y} = \boldsymbol{\alpha}(\boldsymbol{x}) \to 0$, and, from the Eq. (10), $\dot{\boldsymbol{q}} \to 0$, which concludes the proof.

Remark 3 *Assume also that* $V(\boldsymbol{x})$ *is radially unbounded and* $\frac{\partial V(\boldsymbol{x})}{\partial \boldsymbol{x}}(\boldsymbol{f}(\boldsymbol{x}) + G(\boldsymbol{x})\boldsymbol{\alpha}(\boldsymbol{x})) \leq 0,\ \forall \boldsymbol{x} \in \Re^m$, *then the state of the whole system* $[\boldsymbol{x}^T,\ \boldsymbol{q}^T,\ \dot{\boldsymbol{q}}^T]^T$ *is globally bounded and converges to the largest invariant set contained in* $M(\boldsymbol{x}, \boldsymbol{q}, \dot{\boldsymbol{q}})$. *If* $\frac{\partial V(\boldsymbol{x})}{\partial \boldsymbol{x}}(\boldsymbol{f}(\boldsymbol{x}) + G(\boldsymbol{x})\boldsymbol{\alpha}(\boldsymbol{x})) < 0$, *then the equilibrium* $[\boldsymbol{x}^T,\ \boldsymbol{q}^T,\ \dot{\boldsymbol{q}}^T]^T = [\boldsymbol{0},\ \boldsymbol{q}^{T\,*},\ \boldsymbol{0}]^T$ *is quasi-globally asymptotically stable.*

Remark 4 *The above result is quasi-global, in the sense that control law in Eq. (11) is undefined in the points of the state space where the robot Jacobian* $J(\boldsymbol{q})$ *is singular, infact the kinematic inversion is required in computing the expression of* $\overline{\boldsymbol{\alpha}}(\boldsymbol{x}, \boldsymbol{q})$.

4 A case study

In this section, we apply the developed design approach in the case of controlling the pose of the robot camera with respect to a rigid object, assuming affine transformation in the image plane (Allotta *et al.*, 1998). The image-based visual system consists of a PUMA 560 robot arm with a Sony CCD camera mounted on its wrist. It is assumed that the object's visible surface is quasi-planar, with respect to camera frame the surface has equation: $z(x, y) \approx px + qy + c$, and a linear approximation of perspective projection (i.e. weak perspective) is used, with fixed focal length f. It follows that changes in shape are modeled as 2-D affine transformations:

$$\boldsymbol{p}^2 - \boldsymbol{p}_c^2 = A_{12}(\boldsymbol{p}^1 - \boldsymbol{p}_c^1) \quad , \tag{14}$$

where $\{\boldsymbol{p}^1\}$ and $\{\boldsymbol{p}^2\}$ are two image points corresponding to the same object point at time t_1, t_2, and the corresponding centroids of the image patch γ are $\boldsymbol{p}_{\mathrm{C}}^1$ and $\boldsymbol{p}_{\mathrm{C}}^2$. The camera-object interaction is described by the following dynamic model: $\dot{\boldsymbol{w}} = \overline{G}(\boldsymbol{w}, p, q, c)\,\boldsymbol{y}$, where $\boldsymbol{y}$ is the relative velocity twist. The state vector is $\boldsymbol{w} = [p_x^c\ p_y^c\ a_{11}\ a_{12}\ a_{21}\ a_{22}]^{\mathrm{T}} \in \Re^2 \times GL(2)$, the first two components are the centroid coordinate of the image patch γ, whether the others are the elements of matrix A_{12}. The interaction matrix $\overline{G}(\boldsymbol{w}, p, q, c)$ results (Allotta *et al.*, 1998):

$$\begin{bmatrix} \frac{-f}{z_c} & 0 & \frac{p_x^c}{c} & 0 & -f & p_y^c \\ 0 & \frac{-f}{z_c} & \frac{p_y^c}{c} & f & 0 & -p_x^c \\ \frac{a_{11}p+a_{21}q}{c} & 0 & \frac{a_{11}}{c} & 0 & 0 & a_{21} \\ \frac{a_{12}p+a_{22}q}{c} & 0 & \frac{a_{12}}{c} & 0 & 0 & a_{22} \\ 0 & \frac{a_{11}p+a_{21}q}{c} & \frac{a_{21}}{c} & 0 & 0 & -a_{11} \\ 0 & \frac{a_{12}p+a_{22}q}{c} & \frac{a_{22}}{c} & 0 & 0 & -a_{12} \end{bmatrix},$$

where $z_c = c/(1 - p\frac{p_x^c}{f} - q\frac{p_y^c}{f})$ is the centroid depth expressed as function of image coordinates. Denote with $\boldsymbol{w}^{(\mathrm{d})}$ the desired constant state, in the error coordinates $\boldsymbol{x} = \boldsymbol{w} - \boldsymbol{w}^{(\mathrm{d})}$ the visual subsystem has equation: $\dot{\boldsymbol{x}} = G(\boldsymbol{x}, p, q, c)\,\boldsymbol{y}$. By using the control law: $\boldsymbol{y} = \boldsymbol{\alpha}(\boldsymbol{x}) = -G(\boldsymbol{x}, p, q, c)^{-1}\Lambda\boldsymbol{x}$, being Λ a positive definite matrix, then the function $V(\boldsymbol{x}) = \frac{1}{2}\boldsymbol{x}^{\mathrm{T}}\boldsymbol{x}$ satisfies the assumption (1) in a neighbourhood of the point $\boldsymbol{x} = 0$, if the corresponding total relative degree at this point is defined.

The PUMA robot is commanded by a local position controller (MARK III) implementing the inner loop, it operates under VAL II programs and communicates with the PC through the ALTER real time protocol using an RS-232 serial interface. Esperimental study (Buttazzo *et al.*, 1994) has shown that the PUMA robot dynamics compensated by the local position controller can be modeled as a dominant pole linear system for each degree of freedom: $Y_i(s) = \frac{a}{s+a}U_i(s),\ i = 1, ..6$, where s denote the Laplace variable, and $a = 14rad/sec$ is the dominant pole of the robotic system. Hence, the linear subsystem has state space equation:

$\dot{\boldsymbol{\xi}} = A\boldsymbol{\xi} + B\boldsymbol{u}$, $\boldsymbol{y} = H\boldsymbol{\xi}$, where $A = -aI_6$, $B = I_6$, $H = aI_6$, being I_6 the identity matrix. The assumptions of Prop (1) are satisfied, since the linear subsystem has vector realative degree $\{1, \dots, 1\}$, and there is no zero dynamics. We apply the control law (4) to this dynamic look-and-move system, quadratic B-spline active contours are used to track the projection of the image patch (Colombo and Allotta, 1999). A trial is reported in order to show the performance of the proposed control design. The matrix of control gains have been chosen diagonal, namely $\Lambda = \mathrm{diag}(0.1, 0.1, 0.1, 0.1, 0.1, 0.1)$, and $K = \mathrm{diag}(10, 10, 10, 10, 10, 10)$. The initial state is $\boldsymbol{x}_0 = [0\ 0\ 1\ 0\ 0\ 1]^{\mathrm{T}}$, corresponding to the 3-D parameters $p_i = -1.5$, $q_i = -0.86$, and $c_i = 800$. The desired state is $\boldsymbol{x}^{(d)} = [0\ 0\ -0.98\ -2.3\ 3.43\ 0.98]^{\mathrm{T}}$, corresponding to the 3-D parameters $p_f = -0.5$, $q_f = -0.28$, and $c_f = 400$ (there are also dual parameters due to ambiguity). Notice that initial 3-D coefficients can be determined by a predefined open-loop motion of the camera. Plots of the centroid coordinates of γ and of the elements of the matrix A_{12} are shown in Figs. 2.a and Fig. 2.b; Figs. 2.c and Fig. 2.d show 3-D orientation and distance parameters; Fig. 2.e and Fig. 2.f show the components of the requested camera velocity twist. Th desired values are also shown.

The simulation results show the convergence of state error and the asymptotic stability of the whole system as formally proven in Prop. 1. The above result is quasi-global, infact the control law in Eq. (4) is undefined in the points of the state space where also the total relative of the visual subsytem is undefined.

5 Conclusions

The problem of the inclusion of robot dynamics in the control loop of the visual system is solved by applying backstepping approach. A smooth input-affine nonlinear system describes the dynamic visual interaction between the robot camera and the image features, this system is interconnected with the robot manipulator, realizing a dynamic look-and-move system or direct visual servo. In both cases, the designed control system ensures Lyapunov stability and convergence to a local invariant set in the state space. Sufficient conditions which guarantee local and global asymptotic stability around the set of desired image features are provided. As case study, the problem of controlling the pose of the robot camera monted on a 6-DOF manipulator with respect to a rigid object is addressed, and simulation results are reported.

References

Allotta, B., F. Conticelli, and C. Colombo (1998). "Robust decoupling control of an image-based visual system," in *4th IFAC Nonlinear Contr. Syst. Des. Symp., Enschede, The Netherlands.*

Buttazzo, G., B. Allotta, and F. Fanizza (1994). "Robust decoupling control of an image-based visual system," *IEEE Control System.*

Castano, A. and S. Hutchinson (1994). "Visual compliance: task-directed visual servo control," *IEEE Trans. Robot. Autom.*, **10**, pp. 334–342.

Colombo, C. and B. Allotta (1999). "Image-based robot task planning and control using a compact visual representation," *IEEE Trans. on Systems, Man and Cybernetics*, **29**, no. 1, pp. 92–100.

Conticelli, F. and B. Allotta (1998). "Dynamic extension and sliding control in image-based visual servoing," in *IEEE Int. Conf. on Control Applications*, Trieste, Italy.

Corke, P. and M. Good (1996). "Dynamic effects in visual closed-loop systems," *IEEE Trans. Rob. Autom.*, **12**, no. 5, pp. 671–683.

Espiau, B., F. Chaumette, and P. Rives (1992). "A new approach to visual servoing in robotics," *IEEE Trans. Robot. Autom.*, **8**, pp. 313–326.

Feddema, J. and O. Mitchell (1989). "Vision guided servoing with feature-based trajectory generation," *IEEE Trans. Robot. Autom.*, **5**, pp. 691–700.

Grosso, E., G. Metta, A. Oddera, and G. Sandini (1996). "Robust visual servoing in 3-D reaching tasks," *IEEE Trans. Robot. Autom.*, **12**, no. 5, pp. 732–742.

Hashimoto, K., T. Ebine, and H. Kimura (1996). "Visual servoing with hand-eye manipulator-optimal control approach," *IEEE Trans. Robot. Autom.*, **12**, no. 5, pp. 766–774.

Hill, J. and W. T. Park (1979). "Real time control of a robot with a mobile camera," in *Proc. 9th ISIR, Washington, D.C.*, pp. 233–246.

Isidori, A. (1989). *Nonlinear Control Systems: An Introduction*, Springer Verlag.

Kelly, R., R. C. O. Nasisi, B. Kuchen, and F. Reyes (1997). "A stable visual servo controller for camera-in-hand robotic systems," in *8th International Conference onAdvanced Robotics, ICAR '97.*

Koenderink, J. (1986). "Optical flow," *Vision Research*, **26**, no. 1, pp. 161–180.

Krstić, M., I. Kanellakopoulos, and P. Kokotović (1995). *Nonlinear and Adaptive Control Design*, John Wiley & Sons, Inc.

Mundy, J. and A. Zisserman (1992). "Projective geometry for machine vision," in *Geometric Invariance in Computer Vision*, MIT Press.

Papanikolopoulos, N. P. and P. K. Khosla (1993). "Adaptive robot visual tracking: theory and experiments," *IEEE Trans. Autom. Contr.*, **38**, no. 3, pp. 429–445.

Slotine, J. J. and W. Li (1993). *Applied Nonlinear Control*, Prentice Hall, Englewood Cliffs, New Jersey.

Weiss, L., A. Sanderson, and C. Neuman (1987). "Dynamic sensor-based control of robots with visual feedback," *IEEE Journal of Robotics and Automation*, **3**, no. 5, pp. 404–417.

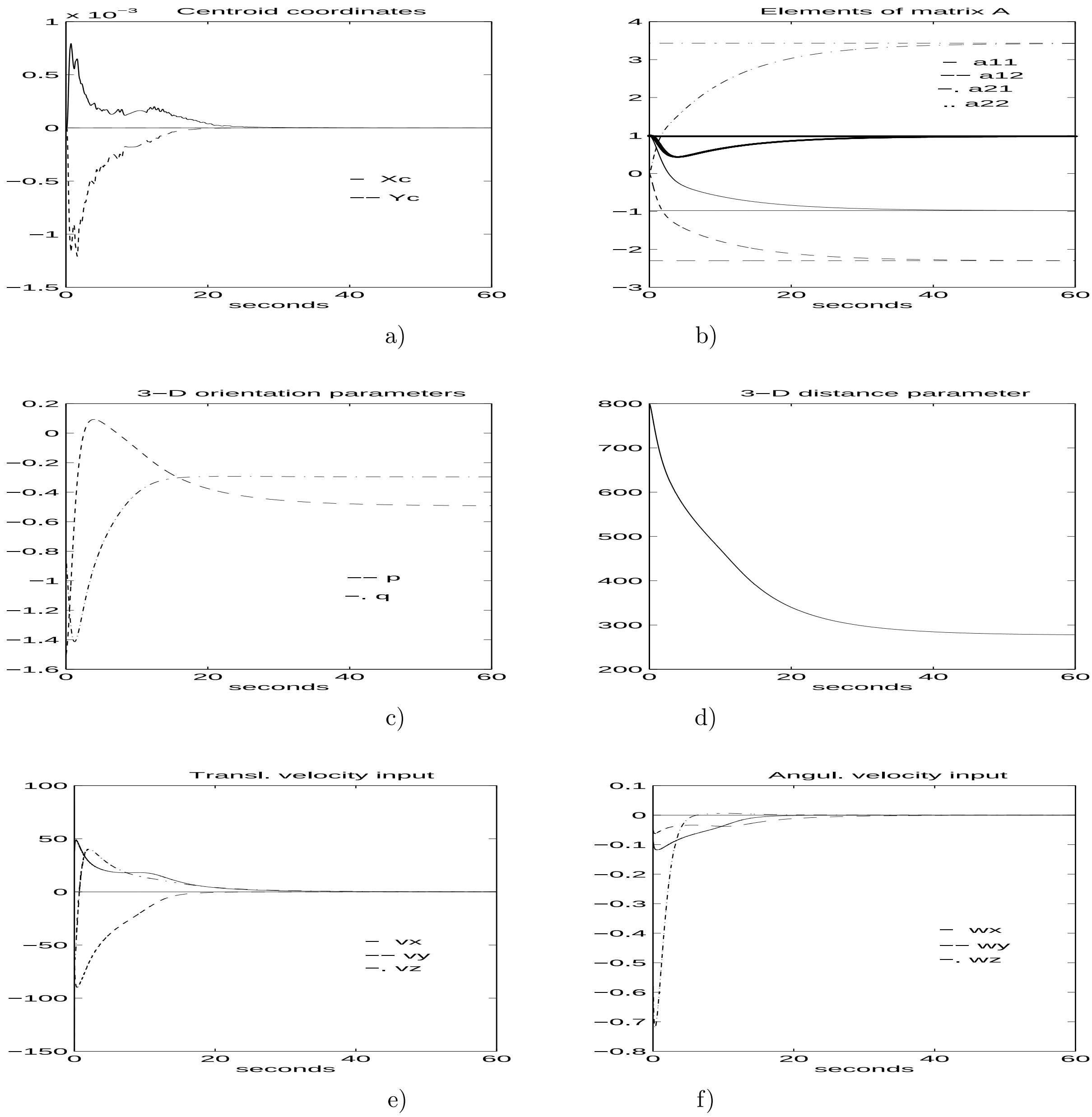

Figure 2: Simulation results: a) centroid coordinates x_c, y_c; b) elements a_{ij}; c) 3-D orientation parameters p, q; d) distance parameter c; e) camera velocity components; d) camera angular velocity components.